APS physics

CHORUS

This is the accepted manuscript made available via CHORUS. The article has been published as:

Higher Order Pancharatnam-Berry Phase and the Angular Momentum of Light

Giovanni Milione, S. Evans, D. A. Nolan, and R. R. Alfano

Phys. Rev. Lett. **108**, 190401 — Published 9 May 2012

DOI: 10.1103/PhysRevLett.108.190401

Higher Order Pancharatnam-Berry Phase and the Angular Momentum of Light

Giovanni Milione[1], S. Evans[1], D. A. Nolan[2], and R. R. Alfano[1*]
[1] *the City College of New York of the City University of New York, 160 Convent Ave. New York, NY 10031*
[2] *Corning Incorporated, Sullivan Park, Corning New York 14831*

The first experimental demonstration of a new Pancharatnam-Berry phase for light beams with spatially inhomogeneous, or vector, states of polarization referred to as the higher-order Pancharatnam-Berry phase is presented. This new geometric phase is proportional to light's total angular momentum, a sum of spin and higher dimensional orbital angular momentum, sharply contrasting the the well known Pancharatnam-Berry phase associated with the plane wave state of polarization of a spatially homogeneous light beam. The higher-order Pancharatnam-Berry phase is directly related to the rotational symmetry of a vortex baring electromagnetic field, associated with the rotational frequency shift of a light beam, and has implications in quantum information science as well as other physical systems such as electron vortex beams.

Since its exposition by Berry in 1984 the Berry phase [1], the phase acquired by a quantum mechanical eigenstate undergoing a cyclic and adiabatic transformation in its parameter space, has become a fundamental and unifying physical concept in numerous and varying fields [2]. This phase is referred to as a geometric phase and, because of its explicit dependence on the geometry of its parameter space, differs markedly from dynamic phase being exceedingly more robust.

Berry's result was the generalization of an earlier result by Pancharatnam in 1955 in the context of a light beam's plane wave state of polarization (SOP) - the Pancharatnam-Berry phase (PBP) [3]. This is illustrated using the corresponding parameter space of the Poincare sphere. The Poincare sphere is the geometric representation of an arbitrary SOP by a sphere where the poles represent right and left circular polarization, equitorial points are linear polarization, and intermediate points between the poles and equator are elliptical polarization [4]. The cyclic transformation of the SOP is equivalent to a closed loop circuit on the PS surface. Upon traversal of the circuit the light beam returns to its initial SOP and acquires the additional PBP which is directly proportional to the area enclosed by the circuit [5]. The PBP is now a well-established phenomenon that has been observed numerous times yet its manifestation has thus far been restricted to light beams whose SOP are spatially *homogeneous* [6].

In this work the first experimental measurement of a new Pancharatnam-Berry phase associated with light beams with a spatially *inhomogenous* or vector SOP is presented. These vector SOP are higher order solutions of Maxwell's equations and we refer to this new geometric phase as a *higher-order* PBP [7]. The higher-order PBP is illustrated using the recently proposed higher-order Poincare sphere representation of a vector SOP [8]. In sharp contrast to the well known PBP the higher-order PBP is shown to be proportional to light's total angular momentum (AM), a sum of the spin and higher dimensional orbital angular momentum.

In an elegant framework Berry showed a state $|\psi(\mathbf{R})\rangle$ undergoing a cyclic transformation over a circuit C with respect to its parameters $\mathbf{R}$ acquires, upon return to it's intial state, an additional phase given by $\gamma(C) = -\int\int_C d\mathbf{S}\cdot\mathbf{V}(\mathbf{R})$. $\mathbf{V}(\mathbf{R}) = \nabla_{\mathbf{R}}\times\mathbf{A}$ plays the role of a 'magnetic field' in the parameter space referred to as the Berry curvature, $\mathbf{A} = \imath\langle\psi(\mathbf{R})|\nabla_{\mathbf{R}}\psi(\mathbf{R})\rangle$ is the associated 'vector potential' referred to as the Berry connection, and $\nabla_{\mathbf{R}}$ is a gradient with respect to the parameters [1]. The phase γ is interpreted as the flux of $\mathbf{V}$ through a surface S enclosed by the a circuit C in the parameter space. In the parameter space of the HOPS, i. e. the sphere's spherical coordinates θ and ϕ, $|\psi(\mathbf{R})\rangle$ is given by

$$|\psi(\theta,\varphi)\rangle = \cos\left(\frac{\theta}{2}\right)|R_\ell\rangle\, e^{\imath\sigma\varphi/2} + \sin\left(\frac{\theta}{2}\right)|L_\ell\rangle\, e^{-\imath\sigma\varphi/2} \tag{1}$$

where $|R_\ell\rangle = (\hat{\mathbf{x}} + \imath\hat{\mathbf{y}})\exp(\imath\ell\varphi/2)/\sqrt{2}$ and $|L_\ell\rangle = (\hat{\mathbf{x}} - \imath\hat{\mathbf{y}})\exp(-\imath\ell\varphi/2)/\sqrt{2}$ are circular polarized phase vortices represented by the poles. The azimuthal phase factor $\exp(\pm\imath\ell\varphi/2)$ is the phase vortex, the optical OAM eigenstates associated with an orbital angular momentum (OAM) per photon of $\ell\hbar$ ($\ell = 0, \pm1, \pm2, ...$), ℓ is the integer number of azimuthal phase windings about the beam axis called the topological charge, and $(\hat{\mathbf{x}}\pm\imath\hat{\mathbf{y}})/\sqrt{2}$ is right and left circular polarization, the optical SAM eigenstates associated with a spin angular momentum (SAM) per photon of $\sigma\hbar$ ($\sigma = \pm1$) [9]. For a paraxial optical beam the SAM and OAM are additive with a total angular momentum (TAM) of $J\hbar = (\ell + \sigma)\hbar$. Eq. 1 describes a vector SOP as represented by the HOPS where the poles are the TAM eigenstates of circular polarized phase vortices, equitorial points are linear polarized vector vortices, and intermediate points between the poles and equator are elliptically polarized vector vortices [8]. The factor of 1/2 in $\exp(\pm\imath\ell\varphi/2)$ is a consequence of exploiting the $2\rightarrow1$ homomorphism between the physical SU(2) space of the light beam and the topological SO(3) space of the HOPS where a rotation of $\varphi/2$ about the beam axis is equivalent to a rotation of φ in the equito-

rial plane of the HOPS.

To find the Berry phase using Eq. 1 each component of the Berry connection $\mathbf{A}$ is evaluated where $\nabla_{\mathbf{R}} = \nabla(\rho, \theta, \varphi)$ is a gradient in spherical coordinates. The components of $\mathbf{A}$ are given by $A_\rho = \langle\psi(\theta,\varphi)|\imath\partial_\rho\psi(\theta,\varphi)\rangle/\rho$, $A_\theta = \langle\psi(\theta,\varphi)|\imath\partial_\theta\psi(\theta,\varphi)\rangle$, and $A_\varphi = \langle\psi(\theta,\varphi)|\imath\partial_\varphi\psi(\theta,\varphi)\rangle/\rho\sin\theta$. Carrying out the derivatives it is easily shown $A_\theta = -\imath\cos(\theta/2)\sin(\theta/2)/2 - \imath\cos(\theta/2)\sin(\theta/2))/2 = 0$ and $A_\rho = 0$. The remaining component A_φ depends explicitly on φ due to the factor $\exp(\pm\imath(\ell+\sigma)\varphi/2)$. Taking the derivative $\imath\partial_\varphi$ which resembles the optical OAM operator [10] gives $A_\varphi = -(\ell+\sigma)(\cos^2(\theta/2) - \sin^2(\theta/2))/2\rho\sin\theta$. The resulting Berry connection is $\mathbf{A} = -(\ell+\sigma)\cos\theta\hat{\boldsymbol{\varphi}}/2\rho\sin\theta$. The resulting Berry curvature then has only one non zero component, $V_\theta = \partial_\theta(\sin\theta A_\varphi)/\rho\sin\theta$, and is given by $\mathbf{V} = (\ell+\sigma)\hat{\boldsymbol{\rho}}/\rho^2$. Finally, taking $d\mathbf{S} = \rho^2\sin\theta d\rho d\theta d\varphi\hat{\boldsymbol{\rho}}$ and evaluating the integral of Eq. 1 where $\int_0^\pi\int_0^{\pi/2}\sin\theta d\rho d\theta d\varphi = \Omega$, the higher order PBP is found to be

$$\gamma(C) = -(\ell+\sigma)\Omega/2, \tag{2}$$

where Ω is the surface area on the HOPS enclosed by the circuit C. Eq. 2 shows the higher order PBP is directly proportional to the TAM of light, a sum of light' SAM and OAM. This result verifies the conjecture of Eq. 15 of [8]. For the case of $\ell = 0$ the higher order PBP reduces to the well known PBP. Berry interpreted the magnetic field $\mathbf{V}$ to be that of a monopole centered at the Poincare sphere origin [3]. The Berry curvature for the higher order PBP is interpreted as a monopole centered at the HOPS origin whose flux is proportional to the TAM of light.

To experimentally introduce the higher order PBP to a light beam a cyclic transformation on the HOPS is physically carried out. The path considered is the geodesic triangle ABA shown in Fig. 1(e) which is a path between the poles. First, a good approximation of a circular polarized phase vortex baring Laguerre-Gaussian (LG_0^ℓ) beam as represented by the north pole A and given by $|\psi(\theta,\varphi)\rangle = |R_\ell\rangle$ is generated according to the experimental setup in Fig. 1 and shown in the first column of Fig. 2(a). To physically carry out the transformations corresponding to the path ABA optical elements that transform both the SAM and OAM of light are employed, namely *spin-orbit* converters - SOC1 and SOC2. These converters consist of the combination of a half wave plate (HWP) and π-cylindrical lens (πCL) mode converter arranged in series as shown in Fig. 1(d). The beam passes through SOC1 where it is transformed into an orthogonal circular polarized phase vortex of opposite topological charge as represented by the south pole B and given by $|\psi(\theta,\varphi)\rangle = |L_\ell\rangle$ [4, 11]. The beam then passes through SOC2 where it is transformed into the original circular polarized phase vortex completing the path ABA and acquiring the additional higher order PBP γ given by $|R'_\ell\rangle = |R_\ell\rangle\exp(\imath\gamma)$. SOC 2 is rotated with respect to SOC 1 at an angle $\Delta\varphi$. This angle is defined as an equal rotation of the πCL mode converter and HWP. Via the SU(2) and SO(3) homomorphism this angle is directly related to the surface area Ω of the HOPS enclosed by ABA according to $2\Delta\varphi = \Omega/2$.

The resulting higher order PBP is measured interferometrically using a modified Mach-Zender interferometer as shown in Fig. 1. Misalignment of the optical elements can introduce an overwhelming dynamic phase. This is reduced by having the reference beam of the interferometer propagate co-linearly through the converters such that any dynamic phase will be equal and cancel [12]. The initial beam is made to be orthogonal to the reference beam, given by $|\psi(\theta,\varphi)\rangle = |L_\ell\rangle$, using an odd number of reflections in the interferometer such that the higher-order PBP of each beam will be opposite and additive. A linear polarizer placed after SOC2 allows the two beams to interfere producing an interferogram given by

$$\begin{aligned} I &\propto (\langle R_\ell|' + \langle L_\ell|')\hat{\mathbf{P}}\hat{\mathbf{P}}(|R_\ell\rangle' + |L_\ell\rangle') \\ &\propto 1 + \cos^2(2\ell\varphi + 2\gamma + 2\alpha) \end{aligned} \tag{3}$$

where $\hat{\mathbf{P}} = \cos\alpha\hat{\mathbf{x}} + \sin\alpha\hat{\mathbf{y}}$ and α is the rotation of the linear polarizer transmission axis. The interferogram described by Eq. 3 is a φ-dependent fringe pattern consisting of 2ℓ intensity lobes. As the term $2\gamma+2\alpha$ is varied the lobes will rotate. Using Eq. 1 and the SU(2) to SO(3) homomorphism 2γ can be expressed as $2\gamma = (\ell+\sigma)4\Delta\varphi$. For a constant polarizer orientation the rotation of the lobes depends on the rotation of SOC2 and the TAM of the light beam. When 2γ is an integer multiple m of 2π a lobe is replaced by an adjacent lobe which is equivalent to a fringe shift. This relationship can be expressed by

$$\Delta\varphi = m\pi/2(\ell+\sigma). \tag{4}$$

Interferograms corresponding to TAM J for different combinations of OAM ℓ and SAM σ as a function of rotation angle $\Delta\phi$ for one fringe shift $m = 1$ are shown in Fig. 2(a). The higher order PBP is measured by verifying Eq. 4. For each combination of ℓ and σ SOC2 is manually rotated until $m = 10$ fringe shifts are observed and the total $\Delta\phi$ recorded. The higher m reduces error associated with 'drift' in the interferometer. It is possible to simultaneously measure the higher-order PBP for TAM values of $-J$ associated with the reference beam by interpreting the observed lobe rotation as $-m$. Experimentally recorded values of $\Delta\varphi$ as a function of $J = (\ell+\sigma)$ is plotted against Eq. 4 in Fig. 2(b) showing excellent agreement with theory. The experiment is repeated multiple times with similar results found each time. It should be noted that the transformations described above as well as other transformations on the HOPS such as between the poles and equator may also be possible using special

optical elements such as q-plates [13] or sub-wavelength diffraction gratings [14]. An analysis of these transformations can be carried out using the Jones matrix formalism for light with both SAM and OAM [15]. This is the subject of future work .

The experimentally verified higher order PBP is markedly different than the well known PBP because of its dependence on light's TAM. This result gives new meaning to other physical phenomenon such as the rotational frequency shift of a light beam which was also shown to depend on light's TAM [16]. For a light beam with no OAM the rotational frequency shift has been interpreted as an evolving PBP on the Poincare sphere [17]. Here the rotational frequency shift for a light beam with both SAM and OAM is interpreted as an evolving higher order PBP on the HOPS. It is the rotational symmetry of a light beam's electric field that gives rise to the rotational frequency shift and the higher order PBP. To illustrate this point instantaneous field distributions, a snapshot in time, for light beams with varying J are shown in Fig. 3. For $J = 0$ ($\ell = 1, \sigma = -1$) the field has 0-fold rotational symmetry and the corresponding higher order PBP is $\gamma = 0$. $J = 2$ corresponds to light beams with ($\ell = 1, \sigma = 1$) and ($\ell = 3, \sigma = -1$), both have 2-fold rotational symmetry, and both have an equal higher order PBP of $\gamma = -\Omega$. In general, light beams that are TAM eigenstates have a J-fold rotational symmetry and a higher order PBP that depends on the TAM J.

Though this experiment has focused on a particular vector SOP represented by the HOPS this result can be generalized to other vector SOP. The optical OAM eigenstates form a complete orthogonal set and it is therefore possible to represent any light beam as their linear combination called spiral harmonics where the beam is said to have a corresponding OAM spectrum [18]. An arbitrary vector SOP can be represented by the linear combination of right circular and left circular polarized spiral harmonics and the constituent components being the TAM eigenstates of circular polarized phase vortices each have an associated higher order PBP.

Due to its robustness and distinction from dynamic phase the geometric phase has found novel applications in quantum information science where for example it has been proposed as a topological phase gate [19]. Exploration of the higher-order PBP as the photonic analog of a topological phase gate for the TAM of light in for example the sorting of single photons [20] as well as its use to manipulate the entanglement [21] my lead to new applications in quantum information science where utilizng the TAM of light allows photonic superdense coding [22] and vector SOPs, of which TAM eigenstates are the constituent components, have received recent interest because they present natural inseperable Bell states of a photon's SAM and OAM degrees of freedom [23].

In conclusion, a new PBP referred to as the higher-order PBP has been theoretically and experimentally presented for the first time. The higher order PBP differs from the well known PBP in that it depends explicitly on the TAM of a light beam and is associated with the rotational symmetry of a light beam's electric field which is tied to other physical phenomena such as the rotational frequency shift of a light beam. This result has important implications for vector SOPs and vortex beams such as the higher order modes of optical fibers but also also in other physical systems such as vortex baring electron beams [24]. This is particularly interesting In the context of a recently proposed spin-orbit conversion of a vortex electron beam because the higher-order PBP would then be related to a real magnetic field [25].

The authors acknowledge financial support from the ARO Grant. No. 52759-PH-H, the NSF GRFP Grant. No. 40017-00-04, and Corning Inc. G M thanks all the participants of the Singular Optics workshop in Trieste, Italy in June 2011 for invaluable discussion and insight.

* giomilione@gmail.com, ralfano@sci.ccny.cuny.edu

[1] M. V. Berry, Proc. R. Soc. Lond. A **392**, 45 (1984).
[2] A. Shapere and F. Wilczek, *Geometric phases in physics* (World Scientific, 1989).
[3] M. V. Berry, J. Mod. Opt. **34**, 1401 (1987).
[4] M. Born and E. Wolf, *Principles of Optics*, 7th ed. (Cambridge University Press, Cambridge, 1999).
[5] S. Pancharatnam, Proc. Ind. Acad. Sci. A **44** (1956).
[6] P. Hariharan (Elsevier, 2005) pp. 149 – 201.
[7] R. H. Jordan and D. G. Hall, Opt. Lett. **19**, 427 (1994).
[8] G. Milione *et al.*, Phys. Rev. Lett. **107**, 053601 (2011).
[9] A. M. Yao and M. J. Padgett, Adv. Opt. Photon. **3**, 161 (2011).
[10] S. van Enk and G. Nienhuis, Opt. Comm.3 **94**, 147 (1992).
[11] M. W. Beijersbergen *et al.*, Optics Communications **96**, 123 (1993).
[12] E. J. Galvez *et al.*, Phys. Rev. Lett. **90**, 203901 (2003).
[13] L. Marrucci *et al.*, Phys. Rev. Lett. **96**, 163905 (2006).
[14] Z. Bomzon, G. Biener, V. Kleiner, and E. Hasman, Opt. Lett. **27**, 285 (2002).
[15] L. Allen *et al.*, Phys. Rev. E **60**, 7497 (1999).
[16] J. Courtial *et al.*, Phys. Rev. Lett. **81**, 4828 (1998).
[17] R. Simon *et al.*, Phy. Rev. Lett. **61**, 19 (1988).
[18] G. Molina-Terriza, J. P. Torres, and L. Torner, Phys. Rev. Lett. **88**, 013601 (2001).
[19] D. Leibfried *et al.*, Nature **422**, 412 (2003).
[20] J. Leach *et al.*, Phys. Rev. Lett. **92**, 013601 (2004).
[21] A. K. Jha *et al.*, Phys. Rev. Lett. **101**, 180405 (2008).
[22] J. T. Barreiro *et al.*, Nat Phys **4**, 282 (2008).
[23] E. Karimi *et al.*, Phys. Rev. A **82**, 022115 (2010).
[24] K. Y. Bliokh *et al.*, Phys. Rev. Lett. **99**, 190404 (2007).
[25] E. Karimi, L. Marrucci, V. Grillo, and E. Santamato, Phys. Rev. Lett. **108**, 044801 (2012).

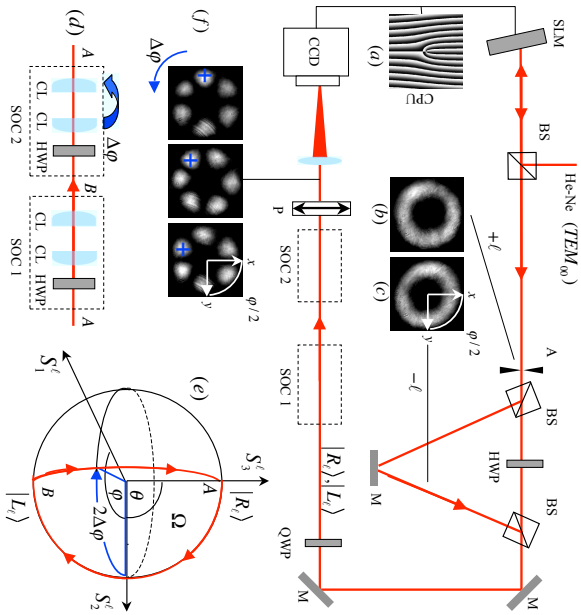

FIG. 1. Experimental setup: A collimated (waist size ~ 5 mm) and linear polarized TEM_{00} mode from a He-Ne laser (632 nm, 5 mW) is converted into a good approximation of phase vortex baring LG_0^{ℓ} mode using a reflective phase only spatial light modulator (SLM) (Holoeye LC-720) displaying a blazed fork grating which controls the OAM. A $LG_0^{-\ell}$ mode (the reference beam) is generated by an odd number of reflections using a modified Mach-Zender interferometer comprised of two beam splitters (BS) and one mirror (M). A HWP and quarter wave plate (QWP), which controls the SAM, are used to give the two beams orthogonal circular polarization. The two beams, given by $|R_\ell\rangle$ and $|L_\ell\rangle$, pass co-linearly through two *spin-orbit* converters, SOC 1 and SOC 2, comprised of a HWP and πCL mode converter arranged in series. The πCL mode converters consist of two CLs ($f = 5mm$) spaced $2f$ apart. The physical transformations of the *spin-orbi* converters correspond to the path ABA on the HOPS. The beams pass through a linear polarizer (P) and are imaged onto a CCD camera producing the interferograms described by Eq. 4. SOC2 is rotated an angle $\Delta\phi$ which is equivalent to a $2\Delta\phi$ equitorial rotation on the HOPS and results in a rotation of the lobes of the interferogram. (a) Fork grating displayed on SLM (b) Intensity of LG_0^{ℓ} mode (c) Intensity of $LG_0^{-\ell}$ mode (d) *spin-orbit* converters (e) Cylic path on HOPS (f) Rotating interferogram.

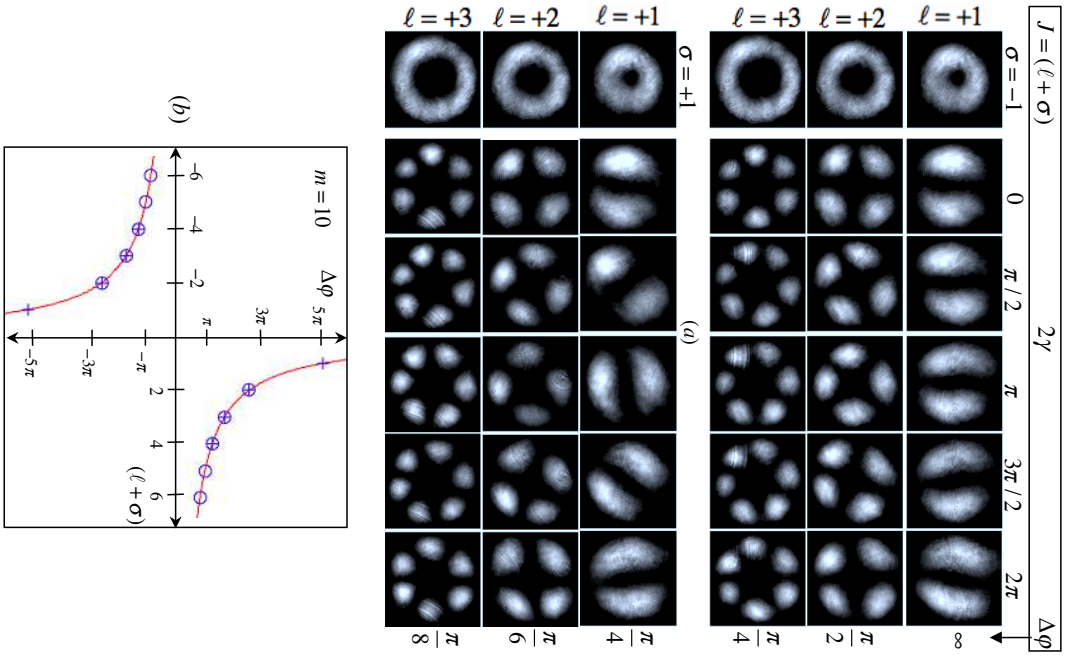

FIG. 2. Experimental Data. (a) Table of interferograms for Eq. 4. Each row displays the observed interferogram lobe rotation for one full fringe shift ($m = 1$) corresponding to the phase shift 2γ in steps of $\pi/2$ for a beam with TAM $J = (\ell + \sigma)$. The total SOC2 rotation $\Delta\varphi$ is shown. (b) Theoretical (red) and experimental (blue) plot of Eq. 5 for $m = 10$ fringe shifts. Crosses represent $sgn(\ell) = sgn(\sigma)$ and circles represent $sgn(\ell) \neq sgn(\sigma)$. Error bars are smaller than the markers.

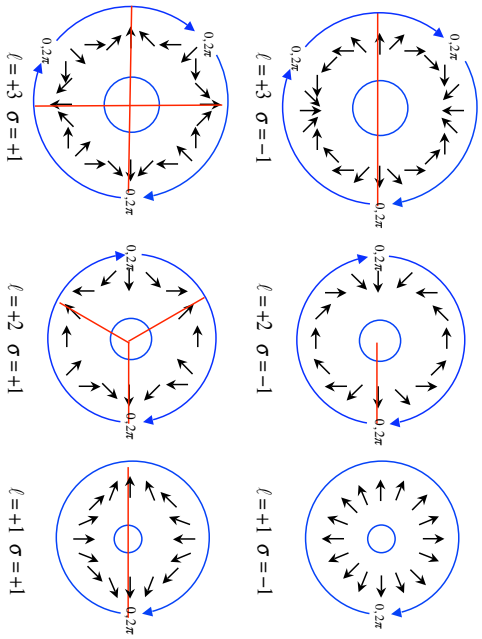

FIG. 3. Instantaneous field distributions, a snapshot in time, for circular polarized phase vortices of TAM $J = (\ell + \sigma)$. Red lines demarcate the field's axis of symmetry.